Very High Bit-Rate Distance Product Using High-Power Single-Mode 850-nm VCSEL With Discrete Multitone Modulation Formats Through OM4 Multimode Fiber

I-Cheng Lu, Chia-Chien Wei, Hsing-Yu Chen, Kuan-Zhou Chen, Cheng-Hsiang Huang, Kai-Lun Chi, Jin-Wei Shi, *Senior Member, IEEE*, Fan-I Lai, Dan-Hua Hsieh, Hao-Chung Kuo, *Fellow, IEEE*, Wei Lin, Shi-Wei Chiu, and Jyehong Chen

Abstract—In order to investigate the tradeoff between optical spectral width and modulation speed of 850-nm Zn-diffusion vertical-cavity surface-emitting laser (VCSEL) and its influence on the performance of discrete multitone (DMT) modulation, two kinds of high-speed VCSEL structures with different cavity lengths ($\lambda/2$ and $3\lambda/2$) are studied. By shortening the cavity length to $\lambda/2$, allocating the oxide layer in the standing-wave peak, and performing a Zn-diffusion aperture in our VCSEL structure, stable dual mode in the output optical spectra across the full range of bias currents with good high-speed performance ($\sim$16-GHz bandwidth) can be achieved. Compared with its multimode reference, it shows far less roll-off with regard to the maximum data rate versus transmission distance over OM4 multimode fibers under forward error correction (FEC) threshold (BER$< 3.8 \times 10^{-3}$). On the other hand, for the $3\lambda/2$ VCSEL structure, by using the same Zn-diffusion conditions as those of dual-mode counterpart, highly single-mode operation (side-mode suppression ratio> 35 dB) with high available power can be achieved over the full range of bias currents. Although such device shows a smaller 3-dB electrical-to-optical bandwidth (12 versus 16 GHz) than that of the dual-mode one, it exhibits a superior transmission performance by use of DMT modulation format. A record high bit-rate distance product (107.6 Gb/s·km) at nearly 50-Gb/s transmission under FEC threshold (BER$< 3.8 \times 10^{-3}$) through 2.2-km OM4 fibers has been successfully demonstrated by the use of single-mode VCSEL with optimized structures. In addition, error-free (BER$< 1 \times 10^{-12}$) transmission at 20.3 Gb/s with bit-rate distance product of 44.66 Gb/s·km has also been demonstrated.

Index Terms—OFDM modulation, semiconductor lasers, vertical cavity surface emitting lasers.

I. Introduction

COST-effective interconnects (OIs) that can be operated at a high bit rate (at least 25 Gb/s by 2020 [1]) across links of >2 km will be needed in modern mega data centers [2]. To date, active optical cables (AOCs) based on 850 nm vertical-cavity surface-emitting lasers (VCSELs) and multimode fibers (MMFs) appear to be the most promising solution for OIs due to the high modulation bandwidth and low power consumption [3]–[7]. By using these VCSELs and simple ON-OFF keying (OOK) modulation, transmission at >40 Gb/s across MMFs has been demonstrated. However, to realize such transmission, both high-speed optical and electrical devices will be necessary, which would thus increase the cost of OIs. Notably, aiming at 400 Gb/s Ethernet, discrete multi-tone (DMT) modulation has been reported as the most cost-effective solution (100 Gb/s × 4 channels) from the view point of optical transmitter/receiver cost reduction [8]. Moreover, compared with pulse-amplitude modulation-4 and OOK modulation, DMT modulation usually has narrower modulation bandwidth, and thus the high-speed ICs (>50 GHz) such as wide-band VCSEL driver and photo-receiver circuit are not necessary. This can further reduce the package and component cost of full AOC module. Except for speed and cost, the power consumption issue is also very important in OIs. Thanks to the remarkable advances in high-performance digital-to-analog converters and analog-to-digital converters, DMT modulation may be considered as a potential solution for OIs due to its increased availability and reduced power consumption [9], [10]. By using a 25G-class VCSEL, optical DMT transmission at >60 Gb/s in the optical back-to-back (OBTB) configuration has been demonstrated [11]. However, the transmitted bit rate drops substantially with an increase in the fiber distance due mainly to the chromatic and modal dispersion of MMFs [11]. It should be noted that the fact that larger modulation bandwidth (>40 GHz) induces more serious dispersion effect, which is the main limitation in the bit-rate distance

product (BRDP). By narrowing down the optical spectral width, single-mode VCSELs have been reported to boost the BRDP, e.g., small aperture VCSELs [5], mode filter VCSELs [12], and photonic crystal VCSELs [13]. For small aperture VCSELs, reducing the diameter of oxide aperture (typically 2∼3 μm) is an effective way to suppress the higher order transverse mode (and consequently narrow down the laser linewidth) and reduce the power consumption as reported in [5]. However, small aperture VCSELs usually have limited output power, which might be insufficient for optical links approaching 2 km. For mode filter VCSELs, surface relief is used to form an integrated mode filter in order to suppress the higher order transverse mode [12]. A BRDP of 40 Gb/s·km (2 km × 20 Gb/s) has been demonstrated using a mode filter VCSEL with multiple oxide layers [12]. The high-power Zn-diffusion single-mode VCSEL is an alternative choice to further boost the value of the BRDP [14]. Compared with the other reported single-mode VCSEL structure outlined above, it can exhibit far lower differential resistance, higher single-mode power, and can eliminate the delicate etching process of top distributed-Bragg-reflector (DBR) layers. Nevertheless, there is usually a tradeoff between VCSEL's modulation speed and its output optical spectral width [14]. The low-frequency roll-off in the single-mode VCSEL induced by serious spatial hole burning usually limits its modulation speed [14]–[16].

In this paper, two kinds of Zn-diffusion high-speed VCSEL structures with different cavity lengths (λ/2 and 3λ/2) are studied in order to investigate the tradeoff between optical spectral width and modulation speed of the Zn-diffusion 850 nm VCSEL and its influence on the performance of DMT modulation. Under the same Zn-diffusion conditions and aperture size, the 3λ/2 cavity VCSEL structure presents superior single-mode characteristics in terms of maximum single-mode output power and side-mode suppression ratio (SMSR) as compared to those of λ/2 counterpart at the expense of smaller modulation speed (12 versus 16 GHz). Although the single-mode device has a narrower 3-dB electrical-to-optical (E-O) bandwidth than that of dual-mode one, it exhibits a superior transmission performance by use of DMT modulation format. Record-high BRDP (107.6 Gb/s·km) at nearly 50 Gb/s transmission under FEC threshold [17] (BER< 3.8 × 10^{-3} [18]) across 2.2 km OM4 fiber has been successfully demonstrated by use of DMT modulation and bit-loading algorithm. These results indicate that judiciously increasing the cavity length (to 3λ/2) can improve the single-mode performance of Zn-diffusion VCESL [14]. Although the modulation speed might be slightly sacrificed for such excellent single-mode performance, the DMT transmission results suggest that single-mode performance (SMSR and power) plays a far more important role in determining the maximum BRDP values than dose modulation speed.

II. DEVICE STRUCTURE AND FABRICATION

Fig. 1(a) and (b) presents the conceptual cross-sectional views of two kinds of devices for high-speed and high-power operations, respectively. These devices have the same top views, as shown in Fig. 1(c). As shown in Fig. 1(a), the epi-layer
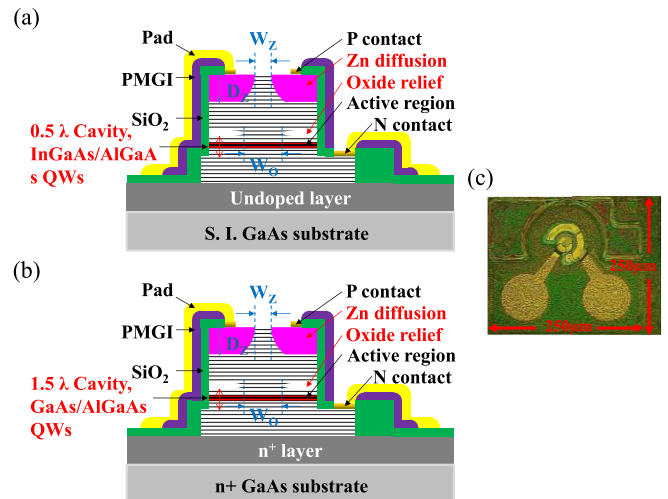

Fig. 1. Conceptual cross-sectional views of (a) high-speed VCSEL on S.I. substrate and (b) high-power VCSEL on n$^+$ GaAs substrate. (c) Top-view of reported devices.

structure for the high-speed (λ/2 thick cavity) VCSEL is composed of three strained In$_{0.08}$Ga$_{0.92}$As/Al$_{0.3}$Ga$_{0.7}$As quantum-wells (QWs) sandwiched between a 36-pair n-type and a 26-pair p-type Al$_{0.9}$Ga$_{0.1}$As/ Al$_{0.12}$Ga$_{0.88}$As DBR layers with an Al$_{0.98}$Ga$_{0.02}$As layer just above the MQWs for electrical and optical confinement (oxidation). The entire structure was grown on a semi-insulating (S.I.) GaAs substrate to mitigate the parasitic RC-limited bandwidth. Here, the cavity length was shortened to λ/2 in order to reduce the internal carrier transient time and increase the optical confinement factor [5]. Strained QWs were employed in the high-speed VCSEL in order to increase the differential gain, and thereby improve the high-speed characteristics of the VCSEL [19].

As shown in Fig. 1(b), the epi-layer structure for the high-power (3λ/2 thick cavity) VCSEL is composed of three unstrained GaAs/Al$_{0.3}$Ga$_{0.7}$As QWs sandwiched between 30-period n-type and 20-period p-type Al$_{0.9}$Ga$_{0.1}$As/Al$_{0.12}$Ga$_{0.88}$As DBR layers with an Al$_{0.98}$Ga$_{0.02}$As layer just above the MQWs for oxidation. There are four major differences in the epi-layer structure between the high-speed and the high-power VCSELs. First, the epi-layer structure is grown on an n$^+$ GaAs substrate, rather than an S.I. substrate. This is because n$^+$ substrates can provide better heat-sinking for high-power operation than that of S.I. substrates. In addition, the parasitic RC-limited bandwidth is not the main factor limiting the modulation bandwidth in high-power single-mode VCSELs. Their speed performance is usually limited by spatial hole burning effect, as discussed in [14]–[16]. Second, cavity length is enlarged to 3λ/2 to dilute the optical confinement and increase the saturation power. Third, we employed GaAs/Al$_{0.3}$Ga$_{0.7}$As QWs in the high-power VCSEL due to their larger density state as compared to that of In$_{0.08}$Ga$_{0.92}$As QWs in the high-speed VCSEL, which might benefit the high-power performance. Fourth, the current-confined layer of the high-power VCSEL is located near a node in the cavity standing wave profile where the optical intra-cavity scattering loss is reduced and thereby improves the high-power
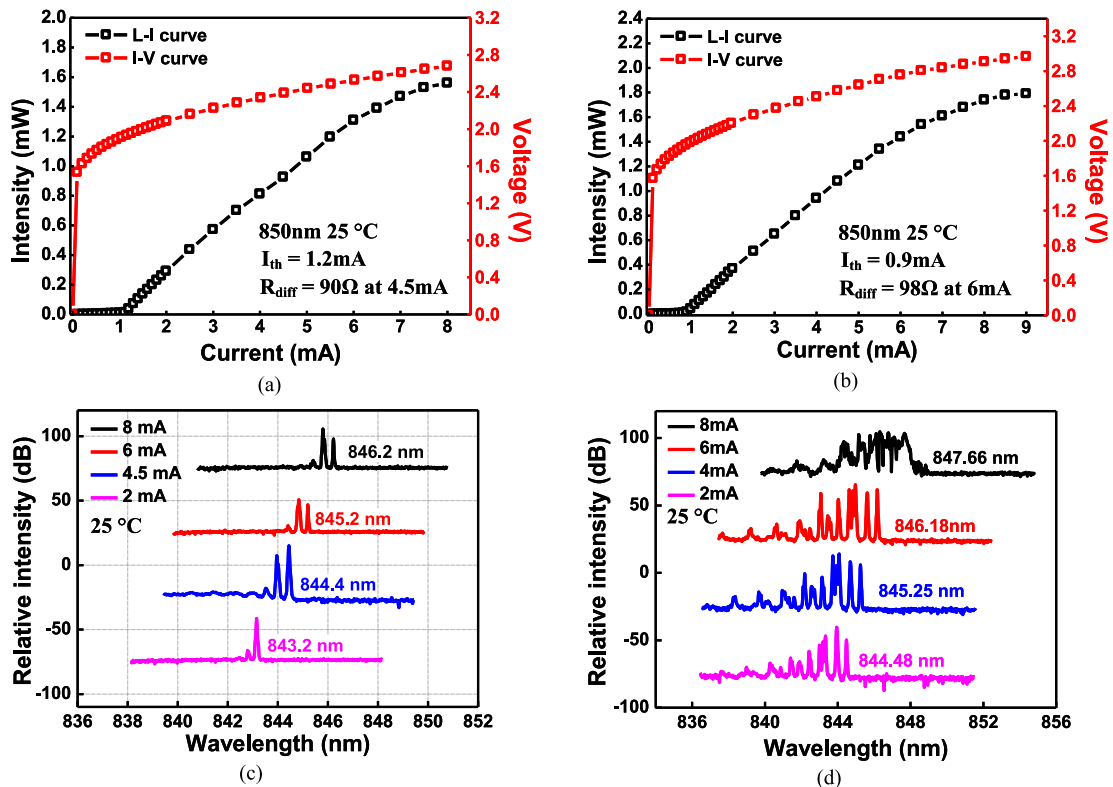
Fig. 2. *L–I–V* characteristics of (a) device A and (b) device B at 25 °C. Optical spectra of (c) device A and (d) device B under various bias currents. (device A: $D_Z/W_Z/W_O = 1.6/6/9$ μm; device B: $D_Z/W_Z/W_O = 1.2/7/7$ μm).

performance. In contrast, for the high-speed VCSEL, the oxide aperture is located at the standing wave peak in the cavity where the optical confinement is increased and thereby benefits its high-speed performance and reduces the threshold current.

Oxide-relief and Zn-diffusion techniques are used in both high-speed and high-power VCSELs. By the use of the chemical solution, the single Al_xO_{1-x} current confined layer is selectively removed without degrading the device performances [7], [14]. Due to the fact that the refractive index of air is much smaller than that of the Al_xO_{1-x} layer (1 versus 1.55), the parasitic capacitance can be further reduced [7]. The Zn-diffusion process is applied to the top DBR of the VCSEL in order to reduce device resistance and manipulate the number of transverse modes [7], [14], [15]. The lasing modes are suppressed by the Zn-diffused DBR region. The threshold gain will become higher due to the increase in free-carrier absorption loss and the decrease in reflectivity after the diffusion (DBR disordering) process [7], [15]. The Zn-diffusion and oxide-relief processes have been explained in more detail elsewhere [7], [14], [15]. During device fabrication, three important parameters can be controlled: D_Z, W_Z, and W_O, representing the Zn-diffusion depth, aperture diameter, and the oxide-relief aperture diameter, respectively. During processing, the high-speed ($\lambda/2$) and high-power ($3\lambda/2$) epitaxial wafers are separately diced into two different pieces for each device structure. Table I lists the cavity lengths and the geometric sizes of high-speed (device A and device B) and high-power (device C and device D) VCSELs.

TABLE I
GEOMETRIC SIZE OF THE STUDIED DEVICES

Device		Cavity	D_Z (μm)	W_Z (μm)	W_O (μm)
High-speed	A[1]	$\lambda/2$	1.6	6	9
	B[1]	$\lambda/2$	1.2	7	7
High-power	C[2]	$3\lambda/2$	1.6	6	9
	D[2]	$3\lambda/2$	1.2	7	4

D_Z: Depth of Zn-diffusion aperture. W_Z: Width of Zn-diffusion aperture.
W_O: Width of oxide-relief aperture.

III. HIGH-SPEED VCSEL

Fig. 1(a) presents a conceptual cross-sectional view of the high-speed VCSEL. Fig. 2(a) and (b) illustrates the power-current-voltage (*L–I–V*) characteristics of high-speed devices A and B at 25 °C, respectively. The threshold current (I_{th}) and differential resistance (R_{diff}) are also specified in Fig. 2(a) and (b). It should be noted that the optical power values presented in this work include a coupling loss of approximately 2 dB between the VCSEL and MMF fiber. As can be seen, by further increasing Zn-diffusion depth (D_Z) and reducing Zn-diffusion aperture diameter (W_Z), device A has higher threshold current (1.2 versus 0.9 mA), lower saturated power (1.6 versus 1.8 mW) and smaller resistance (90 versus 98 Ω) than device B. This is consistent with our previous results [7]. Fig. 2(c) and (d) presents the measured optical spectra of devices A and B under various bias currents at 25 °C. As can be seen, thanks to the Zn-diffusion
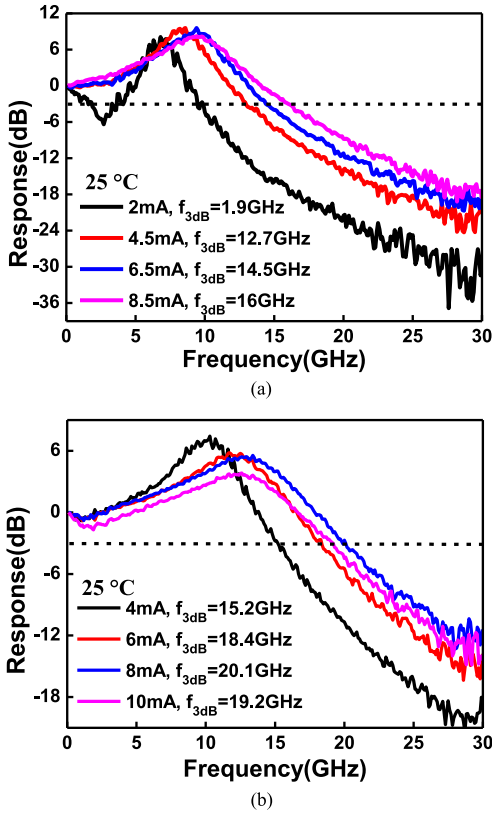
Fig. 3. Measured E-O frequency responses of (a) device A and (b) device B under various bias currents. (device A: $D_Z/W_Z/W_O = 1.6/6/9$ μm; device B: $D_Z/W_Z/W_O = 1.2/7/7$ μm).
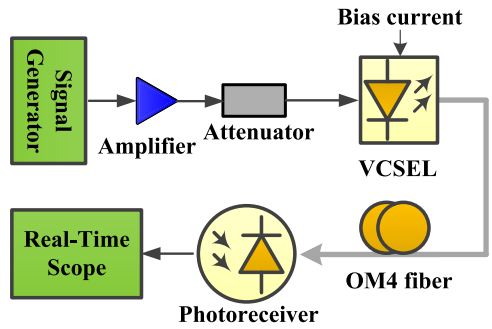

Fig. 4. Experiment setup.

aperture in our VCSEL for optical mode control [7], [14], device A can exhibit dual-mode performance under bias current >4.5 mA even with a large diameter of oxide aperture ($\sim$9 μm), which can benefit the transmission performance. Fig. 3(a) and (b) illustrates the measured E-O responses of devices A and B under various bias currents, respectively. As can be seen, the low-frequency roll-off in typical single-mode VCSEL induced by the spatial hole burning effect [14]–[16] is not significant in our dual-mode VCSEL structure. This can be attributed to a reduction in internal carrier transient time in the short cavity (λ/2). Furthermore, a tradeoff between spectral width and modulation speed can be observed in these two devices (A and B). The maximum modulation speed of devices A and B are 16 and 20 GHz, respectively. For DMT transmission, we optimized the bias cur-
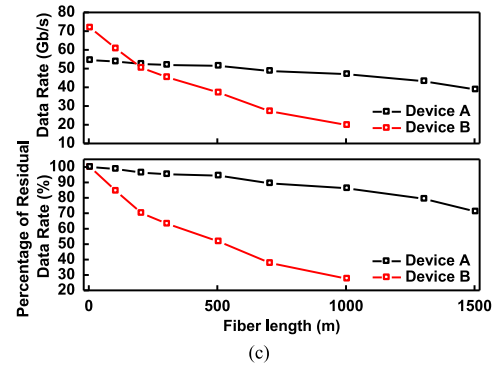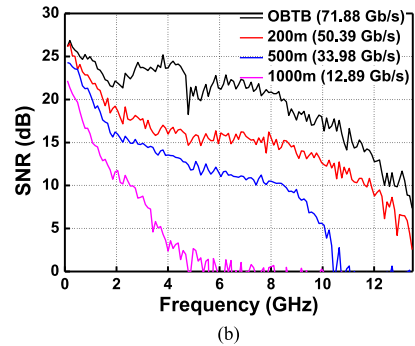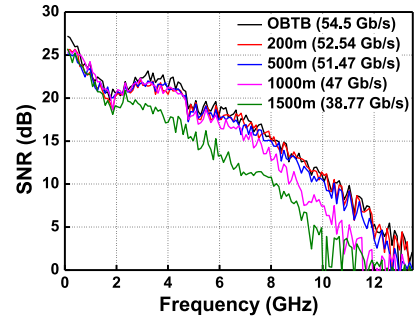

Fig. 5. SNR versus frequency with bit-loading using (a) device A and (b) device B across OM4 fibers and in OBTB configuration. (c) Data rates and percentage of residual data rate versus transmission distance. (device A: $D_Z/W_Z/W_O = 1.6/6/9$ μm; device B: $D_Z/W_Z/W_O = 1.2/7/7$ μm).
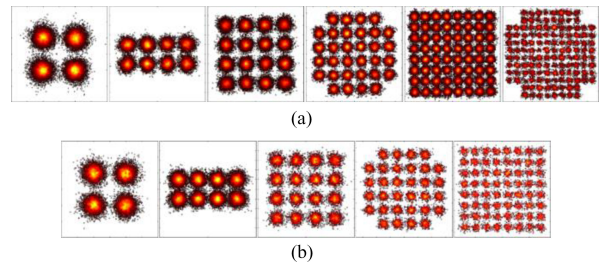
Fig. 6. Constellations of (a) device A and (b) device B after 1 km OM4 fibers. (device A: $D_Z/W_Z/W_O = 1.6/6/9$ μm; device B: $D_Z/W_Z/W_O = 1.2/7/7$ μm).

rents as follows: device A (4.5 mA) and device B (6 mA). It should be noted that the bias currents of the four devices were optimized by running the DMT system over 1 km MMF.

Fig. 4 illustrates the experiment setup of DMT transmission. The baseband electrical DMT signal was generated using offline

Fig. 7. *L–I–V* characteristics of (a) device C and (b) device D at 25 °C. Optical spectra of (c) device C and (d) device D under various bias currents. (Device C: $D_Z/W_Z/W_O = 1.6/6/9\ \mu m$; device D: $D_Z/W_Z/W_O = 1.2/7/4\ \mu m$).
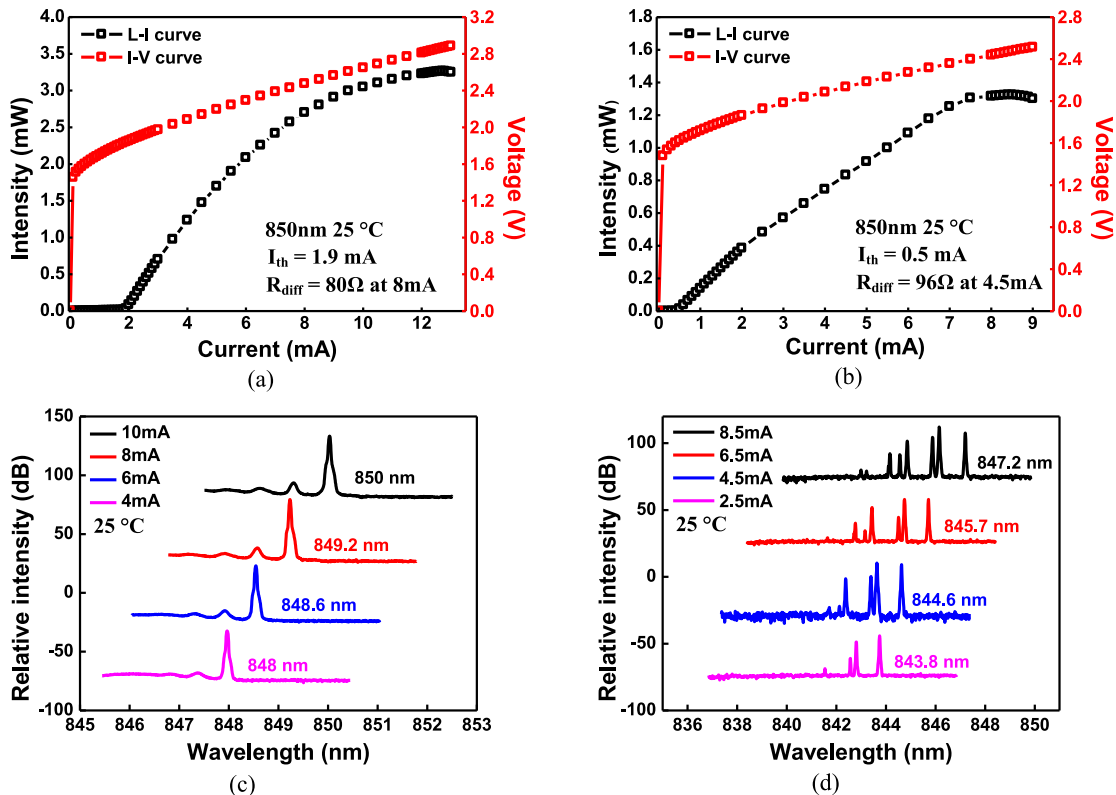
MATLAB with the parameters set as follows: fast Fourier transform size of 512, cyclic prefix of 1.5%, and the subcarrier number of 138. The electrical DMT signal was then generated using an arbitrary waveform generator (Tektronix AWG70001A) at a sampling rate of 50 GSample/s corresponding to a signal bandwidth of 13.5 GHz, and the digital-to-analog conversion resolution and the output peak-to-peak voltage (V_{pp}) were 10 bit and 500 mV, respectively. An electrical amplifier (Picosecond 5867) and an attenuator were used to optimize the optical modulation index for each device. The DMT signal was fed into the high-speed VCSELs through a 26.5 GHz bias-T (Agilent 11612A) via a GS probe. The output light was butt-coupled into a lensed fiber with a core diameter of 62.5 μm and coupling efficiency of approximately 60%. After the OM4 fiber transmission, the optical DMT signal was directly detected using a 9.5 GHz photoreceiver (PICOMETRIX PT-12B). The DMT signal was retrieved and digitized using a real-time oscilloscope (Tektronix DSA71604) with a sample rate of 50 GSample/s and a 3-dB bandwidth of 16 GHz. Demodulation was performed using offline MATLAB DSP programs. The signal-to-noise ratio (SNR) was estimated after demodulation, and the BERs were measured based on a bit-by-bit comparison between transmitted and received data.

Fig. 5(a) and (b) plots the SNR versus frequency of the DMT signal with bit-loading using device A and device B over various transmission distances, respectively. By combining DMT modulation with bit-loading algorithm, we can maximize the data rate and maintain the BER below the FEC threshold of 3.8×10^{-3}. The achieved data rates over various transmission distances are listed in Fig. 5(a) and (b). By the use of device A, the achieved BRDPs are 47 and 58.2 Gb/s·km for 1 and 1.5 km OM4 fibers, respectively. Fig. 5(c) presents the data rates and the percentage of residual data rate versus transmission distance. As can be seen, device A achieves a better transmission (>200 m) performance than device B due to its smaller number of transverse modes. In addition, data rates were shown to drop more with an increase in transmission distance >1 km, due to the serious chromatic and modal dispersion of MMFs, as shown in Fig. 5(c). These DMT transmission results suggest that reducing the number of transverse modes and ultimately achieving single-mode behavior may be the key to extending transmission distance (>2 km OM4 fibers) and achieving a higher BRDP. Fig. 6(a) and (b) shows the constellations for device A and device B after 1 km OM4 fibers.

IV. HIGH-POWER VCSEL

In order to extend the maximum transmission distance in OM4 fibers (>2 km [2]), we sought to optimize the geometric sizes (D_Z, W_Z, and W_O) of our VCSELs with the objective of achieving high-power, single-mode performance. The key to achieving single-mode performance is the suppression of high-order transverse modes in the current-confined region of the VCSEL cavity by employing a Zn-diffusion aperture. Therefore, we must let $W_O > W_Z$ to cause a significant Zn-diffusion induced loss in the current-confined regime. As described in our
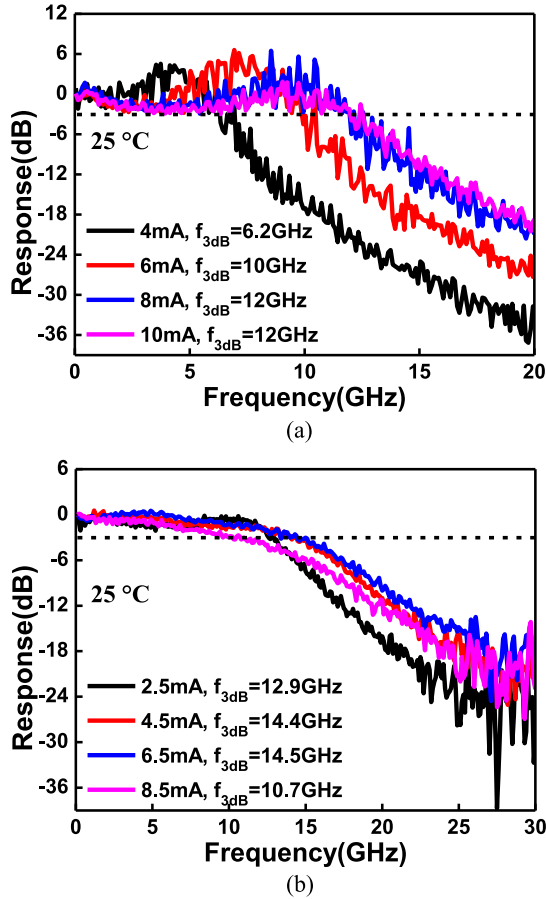
Fig. 8.   Measured E-O frequency responses of (a) device C and (b) device D under various bias currents. (Device C: $D_Z/W_Z/W_O = 1.6/6/9$ μm; device D: $D_Z/W_Z/W_O = 1.2/7/4$ μm).

mode one, due to its much longer coherent time [20]. In order to suppress the feedback effect, an optical isolator is usually integrated with a single-mode laser during high-speed operations and data transmission [21]. As shown in Fig. 8(b), device D has a reasonable maximum 3-dB E-O bandwidth ($\sim$14.5 GHz), despite its low threshold current. Again we can see the tradeoff between spectral width and modulation speed, as in the cases of devices A and B. The fact that the E-O bandwidth of the single-mode device is smaller than that of the MM reference has been attributed to less damping in its E-O frequency response and more serious low-frequency roll-off [14], [16], [22]. A more detailed theoretical [23] work to investigate such phenomenon would be our future work. For DMT transmission, we choose 8 and 4.5 mA for devices C and D, respectively. It should be noted that these bias currents were also optimized using the methods outlined above.

The experiment setup for the high-power VCSEL resembles that of the high-speed VCSEL. Fig. 9(a) and (b) presents the SNR versus frequency of the DMT signal with bit-loading using device C and device D over various transmission distances, respectively. The achieved data rates over various transmission distances are listed in Fig. 9(a) and (b). By using our high-power single-mode VCSEL (device C), we have successfully achieved a record-high BRDP of 107.6 Gb/s·km (2.2 km × 48.92 Gb/s) with BER of $< 3.8 \times 10^{-3}$. Fig. 9(c) presents the data rates and percentage of residual data rate versus transmission distance. By using device C, it shows very small roll-off in the maximum data rate with an increase in transmission distance due to its highly single-mode performance. Fig. 10(a) and (b) presents the constellations for devices C and D after 2.2 km and 1 km OM4 fibers, respectively.

We also demonstrate error-free transmission (defined as a BER of $< 1 \times 10^{-12}$) for device C. The bias current is fixed at 8 mA. Fig. 11(a) presents the SNR versus frequency of the DMT signal with bit-loading using device C. By using bit-loading algorithm, the employed signal bandwidth was decreased to $\sim$8.5 GHz due to the lower target BER. A BRDP as high as 44.66 Gb/s·km (2.2 km × 20.3 Gb/s) was successfully achieved with BER of $< 1 \times 10^{-12}$. It should be noted that the error-free performance was confirmed by measured SNR due to the difficulties associated with direct measurement of such small BER values. To the best of our knowledge, BRDP of 44.66 Gb/s·km is the highest reported for error-free (BER $< 1 \times 10^{-12}$) operations [12]. Fig. 11(b) presents the data rates and percentage of residual data rate versus transmission distance. As can be seen, the data rate also drops at a very slow rate with an increase in fiber distance. Fig. 11(c) presents the constellations of device C for 2.2 km error-free transmission in OM4 fiber.

previous work [14], the Zn-diffusion aperture diameter (W_Z) in the epi-layer structure must be smaller than 6.5 μm to ensure single-mode performance. The geometric sizes (D_Z, W_Z, and W_O) of device C and device D are listed in Table I. Fig. 7(a) and (b) illustrates the L-I-V characteristics of devices C and D at 25 °C, respectively. As can be seen, device C exhibits small differential resistance ($\sim$80 Ω), reasonable threshold current (1.9 mA) and large saturated power ($\sim$3.3 mW) as compared to device D, which can be attributed to the optimization in the geometric sizes of the VCSEL structure. Fig. 7(c) and (d) presents the measured optical spectra of device C and device D under various bias currents at 25 °C, respectively. As can be seen, device C can maintain single-mode performance with SMSR of >35 dB under a full range of bias currents. Fig. 8(a) and (b) illustrates the measured E-O responses of device C and device D under various bias currents, respectively. A reasonable high-speed performance ($\sim$12 GHz) with minimal low-frequency roll-off can be achieved using device C. Minimization of the low-frequency roll-off induced by spatial hole burning can be attributed to the optimization of the geometric structure in our Zn-diffused VCSEL, as discussed in our previous work [14]. In addition, the ringing in measured traces of this highly single-mode device can be attributed to the optical feedback effect, which should be more significant in the single-mode device than the multi-

V. Conclusion

In summary, we have demonstrated optical DMT transmission using two kinds of Zn-diffusion 850 nm VCSELs with different cavity lengths (λ/2 and 3λ/2). By shortening the cavity length to λ/2, placing a current-confined layer to the peak in the cavity standing wave profile, and performing Zn-diffusion process, the dual-mode performance can be achieved under

(a)

(b)

Fig. 10.   Constellations of (a) device C after 2.2 km OM4 fibers and (b) device D after 1 km OM4 fibers. (Device C: $D_Z/W_Z/W_O = 1.6/6/9$ μm; device D: $D_Z/W_Z/W_O = 1.2/7/4$ μm).
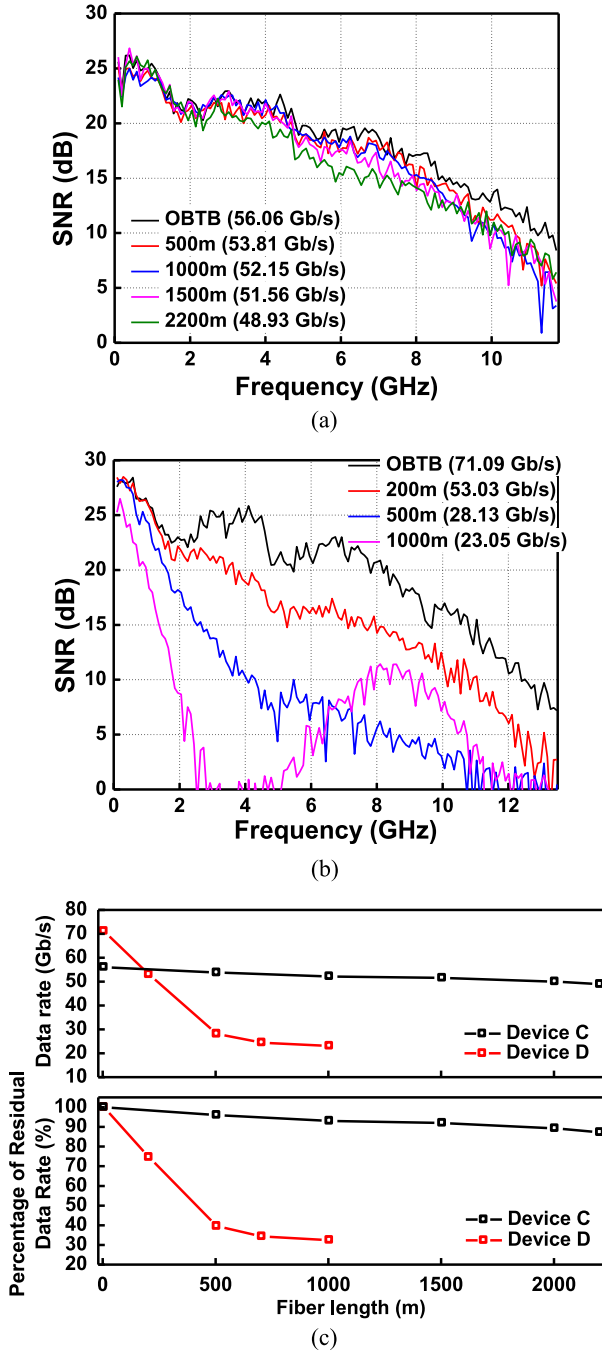

(a)

(b)

(c)

Fig. 9.   SNR versus frequency with bit-loading using (a) device C and (b) device D through OM4 fibers and in OBTB configuration. (c) Data rates and percentage of residual data rate versus transmission distance. (Device C: $D_Z/W_Z/W_O = 1.6/6/9$ μm; device D: $D_Z/W_Z/W_O = 1.2/7/4$ μm).

(a)

(b)

(c)
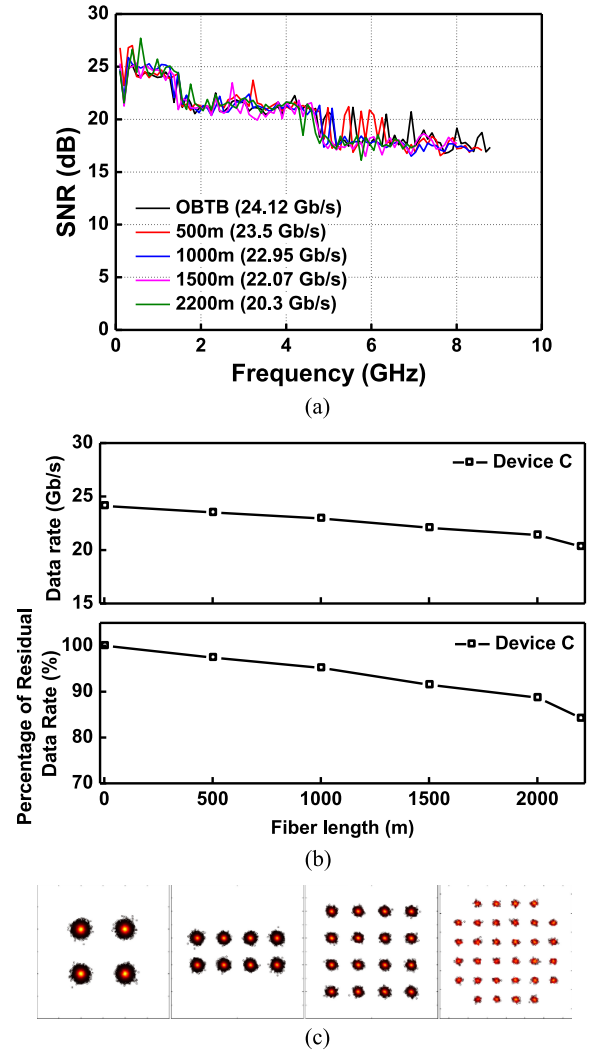
Fig. 11.   SNR versus frequency using device C for error-free transmission through OM4 fibers and in OBTB configuration. (b) Data rates and percentage of residual data rate versus transmission distance. (c) Constellations of device C across 2.2 km OM4 fiber. (Device C: $D_Z/W_Z/W_O = 1.6/6/9$ μm).

a full range of bias currents with high 3-dB E-O bandwidth (16 GHz). Compared with the multimode reference, it shows far less roll-off in the maximum data rate with an increase in transmission distance. On the other hand, by applying the same Zn-diffusion conditions, a high-power (>3 mW) highly single-mode (SMSR> 35 dB) VCSEL with 3λ/2 thick cavity can be achieved. Thanks to its excellent single-mode performance, record-high BRDP (107.6 Gb/s·km) at nearly 50 Gb/s

transmission at BER< 3.8×10^{-3} across 2.2 km OM4 fiber has been successfully achieved by using DMT modulation with bit-loading algorithm. Although the modulation speed might be slightly sacrificed to achieve such excellent single-mode performance, the DMT transmission results suggest that single-mode performance is far more important than high modulation

speed with regard to achieving high BRDP. For the error-free ($BER< 1 \times 10^{-12}$) DMT transmission, a record-high BRDP (44.66 Gb/s·km) has also been successfully demonstrated.

REFERENCES

[1] M. A. Taubenblatt, "Optical interconnects for high-performance computing," *J. Lightw. Technol.*, vol. 30, no. 4, pp. 448–458, Feb. 2012.

[2] C. F. Lam *et al.*, "Fiber optic communication technologies: What's needed for datacenter network operations," *IEEE Commun. Mag.*, vol. 48, no. 7, pp. 32–39, Jul. 2010.

[3] D. M. Kuchta *et al.*, "64Gb/s transmission over 57m MMF using an NRZ modulated 850nm VCSEL," presented at the Optical Fiber Commun. Conf. Exhib., San Francisco, CA, USA, Mar. 2014, Paper Th3C. 2.

[4] P. Westbergh *et al.*, "High-Speed 850 nm VCSELs with 28 GHz modulation bandwidth operating error-free up to 44 Gbit/s," *Electron. Lett.*, vol. 48, no. 18, pp. 1145–1147, Aug. 2012.

[5] P. Moser *et al.*, "Energy-efficient oxide-confined high-speed VCSELs for optical interconnects," *Proc. SPIE, Vertical-Cavity Surface Emitting Lasers*, vol. 9001, pp. 900103-1–900103-8, Feb. 2014.

[6] P. Wolf *et al.*, "Energy efficient 40 Gbit/s transmission with 850 nm VCSELs at 108 fJ/bit dissipated heat," *Electron. Lett.*, vol. 49, no. 10, pp. 666–667, May 2013.

[7] J.-W. Shi, J.-C. Yan, J.-M. Wun, J. J. Chen, and Y.-J. Yang, "Oxide-relief and Zn-diffusion 850 nm vertical-cavity surface-emitting lasers with extremely low energy-to-data-rate ratios for 40 Gbit/sec operations," *IEEE J. Sel. Topics Quantum Electron.*, vol. 19, no. 2, art. no. 7900208, Mar./Apr. 2013.

[8] H. Isono *et al.* (2014, May). DMT relative cost consideration. *IEEE P802.3bs 400 Gb/s Ethernet Task Force*. [Online]. Norfolk, VA, USA. Available: http://www.ieee802.org/3/bs/public/14_05/isono_3bs_02_0514.pdf

[9] R. Bouziane *et al.*, "Design studies for ASIC implementations of 28 GS/s optical QPSK- and 16-QAM-OFDM transceivers," *Opt. Exp.*, vol. 19, pp. 20857–20864, Oct. 2011.

[10] P. A. Milder *et al.*, "Design and simulation of 25 Gb/s optical OFDM transceiver ASICs," *Opt. Exp.*, vol. 19, pp. B337–B342, Dec. 2011.

[11] I. Lyubomirsky, W. A. Ling, R. Rodes, H. M. Daghighian, and C. Kocot, "56 Gb/s transmission over 100 m OM3 using 25G-class VCSEL and discrete multi-tone modulation," presented at the Proc. Optical Int. Conf., San Diego, CA, USA, May 2014, Paper TuC2.

[12] R. Safaisini, E. Haglund, P. Westbergh, J. S. Gustavsson, and A. Larsson, "20 Gbit/s data transmission over 2 km multimode fibre using 850 nm mode filter VCSEL," *Electron. Lett.*, vol. 50, no. 1, pp. 40–42, Jan. 2014.

[13] M. P. Tan *et al.*, "Error-Free transmission over 1-km OM4 multimode fiber at 25 Gb/s using a single mode photonic crystal vertical-cavity surface-emitting laser," *IEEE Photon. Technol. Lett.*, vol. 25, no. 18, pp. 1823–1825, Sep. 2013.

[14] Jin-Wei Shi *et al.*, "Single-mode, high-speed, and high-power vertical-cavity surface-emitting lasers at 850 nm for short to medium reach (2 km) optical interconnects," *J. Lightw. Technol.*, vol. 31, no. 24, pp. 4037–4044, Dec. 2013.

[15] J.-W. Shi, C.-C. Chen, Y.-S. Wu, S.-H. Guol, and Y.-J. Yang, "High-power and high-speed Zn-diffusion single fundamental-mode vertical-cavity surface-emitting lasers at 850 nm wavelength," *IEEE Photon. Technol. Lett.*, vol. 20, no. 13, pp. 1121–1123, Jul. 2008.

[16] J. S. Gustavsson, Å. Haglund, J. Bengtsson, P. Modh, and A. Larsson, "Dynamic behavior of fundamental-mode stabilized VCSELs using shallow surface relief," *IEEE J. Quantum Electron.*, vol. 40, no. 6, pp. 607–619, Jun. 2004.

[17] ITU, "Forward error correction for high bit-rate DWDM submarine systems," ITU-T Recommendation G.975.1, Appendix I.9, 2004.

[18] J. Cho, C. Xie, and P. J. Winzer, "Analysis of soft-decision FEC on non-AWGN channels," *Opt. Exp.*, vol. 20, no. 7, pp. 7915–7928, Mar. 2012.

[19] E. P. O'Reilly and A. R. Adams, "Band-structure engineering in strained semiconductor lasers," *IEEE J. Quantum Electron.*, vol. 30, no. 2, pp. 366–379, Feb. 1994.

[20] P. B. Subrahmanyam, Y. Zhou, L. Chrostowski, and C. J. Chang-Hasnain, "VCSEL tolerance to optical feedback," *Electron. Lett.*, vol. 41, no. 21, pp. 1178–1179, Oct. 2005.

[21] A. Murata and S. Aoki, "A DFB-LD module integrated with 60 db optical isolator for coherent lightwave transmission systems," *IEEE Photon. Technol. Lett.*, vol. 1, no. 8, pp. 221–223, Aug. 1989.

[22] J.-W. Shi, C.-C. Chen, Y.-S. Wu, S.-H. Guol, and Y.-J. Yang, "The influence of Zn-diffusion depth on the static and dynamic behaviors of Zn-diffusion high-speed vertical-cavity surface-emitting lasers at a 850 nm wavelength," *IEEE J. Quantum, Electron.*, vol. 45, no. 7, pp. 800–806, Jul. 2009.

[23] Y. Liu, W.-C. Ng, B. Klein, and K. Hess, "Effects of the spatial nonuniformity of optical transverse modes on the modulation response of vertical-cavity surface-emitting lasers," *IEEE J. Quantum Electron.*, vol. 39, no. 1, pp. 99–108, Jan. 2003.

I-Cheng Lu received the M.S. degree in electrooptical engineering from National Taipei University of Technology, Taipei, Taiwan, in 2010. In 2010, he joined the Institute of Electro-Optical Engineering, National Chiao Tung University, Hsinchu, Taiwan, where he is currently working toward the Ph.D. degree. His research interests include advanced modulation formats and short-range optical communications.

Chia-Chien Wei received the Ph.D. degrees in electrooptical engineering from National Chiao Tung University, Hsinchu, Taiwan, and in electrical engineering from the University of Maryland, Baltimore, MD, USA, in 2008.

In 2011, he joined National Sun Yat-sen University, Kaohsiung, Taiwan, where he is currently an Assistant Professor of the Department of Photonics. His current research interests include optical and electrical signal processing, advanced modulation formats, optical access networks, and radio-over-fiber systems.

Hsing-Yu Chen received the Masters' degree in electrooptical engineering from the National Chiao Tung University, Hsinchu, Taiwan, in 2009, where he is currently working toward the Ph.D. degree with the Department of Photonics. He is an Engineer of the Information and Communications Research Labs, Industrial Technology Research Institute, Taiwan.

Kuan-Zhou Chen is currently working toward the M.S. degree with the Department of Photonics, National Sun Yat-sen University, Kaohsiung, Taiwan.

Cheng-Hsiang Huang is currently working toward the M.S. degree with the Institute of Electro-Optical Engineering, National Chiao Tung University, Hsinchu, Taiwan. His research interest includes short-range optical communications.

Kai-Lun Chi was born in New Taipei City, Taiwan, on February, 10, 1988. He is currently working toward the Ph.D. degree with the Department of Electrical Engineering, National Central University, Taoyuan, Taiwan. His current research interests include high-speed optoelectronic device measurement and high-speed VCSELs and LEDs for the application of optical interconnects.

Jin-Wei Shi (SM'10) was born in Kaohsiung, Taiwan, on January 22, 1976. He received the B.S. degree in electrical engineering from National Taiwan University, Taipei, Taiwan, in 1998, and the Ph.D. degree from the Graduate Institute of Electro-Optical Engineering, National Taiwan University, in 2002. He was a Visiting Scholar at the University of California, Santa Barbara (UCSB), CA, USA, during 2000 and 2001. From 2002 to 2003, he was a Postdoctoral Researcher at the Electronic Research and Service Organization of Industrial Technology Research Institute. In 2003, he joined the Department of Electrical Engineering, National Central University, Taoyuan, Taiwan, where he is currently a Professor. In 2011, he joined the ECE Department of UCSB again as a Visiting Scholar. He has authored or coauthored more than 110 journal papers, 160 conference papers, and holds 20 patents. His current research interests include ultrahigh-speed/power optoelectronic devices, such as photodetectors, electroabsorption modulator, submillimeter-wave photonic transmitter, and semiconductor laser. He was the Invited Speaker of the 2002 IEEE LEOS, the 2005 SPIE Optics East, the 2007 Asia-Pacific Microwave Photonic conference, the 2008 Asia Optical Fiber Communication and Optoelectronic Exposition and Conference, the 2011 Optical Fiber Communication (OFC), and the 2012 IEEE Photonic Conference. He was with the Technical Program Committee of the OFC from 2009 to 2011, 2012 SSDM, 2012 MWP, and 2013 Asia-Pacific CLEO. He received the 2007 Excellence Young Researcher Award from the Association of Chinese IEEE and the 2010 Da-You Wu Memorial Award.

Wei Lin was born in Tainan, Taiwan, on January 11, 1956. He received the B.S. degree from the Tatung Institute of Technology, Chiayi, Taiwan, in 1978, and the M.S. and Ph.D. degrees from National Cheng-Kung University, Tainan, all in electrical engineering.

From 1981 to 1991, he was an Engineer at the Northern Taiwan Telecommunications Administration, Ministry of Transportation and Communications. From 1991 to 1998, he was with the Photonic Technology Research Laboratory of Chung-Hwa Telecommunication Laboratories (CHTL), Ministry of Transportation and Communications as a Task Leader and then been promoted to a Project Leader in 1992. In 1998, he left CHTL and founded LandMark Optoelectronics Corporation (LMOC) producing InP- and GaAs-based epiwafers by MOVPE technology. LMOC's epiwafers are mainly applied to optical fiber communications. He was the Vice President in LMOC during 1998 to 2005 and has been promoted to the General Manager since 2005. He has also been the Leader of the Research and Developing Group in LandMark since 2011. He has been working on metalorganic vapor phase epitaxy (MOVPE) for 23 years. His research interests include growth and characterization of III–V compound semiconductors, fabrication and characterization of modulation-doped pseudomorphic AlGaInAs/(In)GaAs or AlGaAs/(In)GaAs FET's, many kinds of InGaAsP//InP or AlGaInAs/InP long-wavelength lasers (1.2–1.9 m), InGaAs/InP photodetectors and GaAs-based material high-power lasers and vertical-cavity surface-emitting laser.

Dr. Lin is a Member of the Taiwan Chinese Society for Materials Science.

Fan-I Lai received the M.S. and the Ph.D. degrees from the Institute of Electro-Optical Engineering, National Chiao-Tung University, Hsinchu, Taiwan, in 2001 and 2005, respectively. Since 2007, she is with Yuan Ze University as a Faculty Member of the Department of Electrical Engineering. Her current research interests include vertical-cavity surface-emitting lasers, blue and UV lasers and LED, quantum-confined optoelectronic structures, and nanostructure applications.

Shi-Wei Chiu received the B.S. and M.S. degrees in electrical engineering from National Cheng Kung University, Tainan, Taiwan, in 1992 and 1994, respectively, and the Ph.D. degree in electrical engineering from National Chiao Tung University, Hsinchu, Taiwan, in 2000.

He joined LandMark Optoelectronics Corporation, Tainan, in 2012, where he has been working on the research and development of semiconductor lasers.

Dan-Hua Hsieh received the M.S. degree in electrooptical engineering from Yuan-Ze University, Taoyoung, Taiwan, in 2012. He is currently working toward the Ph.D. degree with the Institute of Electro-Optical Engineering, National Chiao Tung University, Hsinchu, Taiwan, since 2012. His research interest includes the design and fabrication of VCSEL devices.

Hao-Chung Kuo (S'98–M'99–SM'06–F'14) received the B.S. degree in physics from National Taiwan University, Taipei, Taiwan, the M.S. degree in electrical and computer engineering from Rutgers University, New Brunswick, NJ, USA, in 1995, and the Ph.D. degree from the University of Illinois at Urbana Champaign, Urbana, IL, USA, in 1999. He has an extensive professional career both in research and industrial research institutions that includes: Research Assistant at Lucent Technologies, Bell Laboratories, from 1993 to 1995; and a Senior R&D Engineer in Fiber-Optics Division at Agilent Technologies from 1999 to 2001 and at LuxNet Corporation from 2001 to 2002. Since October 2002, he has been with the National Chiao Tung University (NCTU) as a Faculty Member of the Institute of Electro-Optical Engineering. He is currently the Associate Dean, Office of International Affair, NCTU. He has authored and coauthored 300 international journal papers, two invited book chapter, six granted and 12 pending patents. His current research interests include semiconductor lasers, VCSELs, blue and UV LED lasers, quantum-confined optoelectronic structures, optoelectronic materials, and solar cell. He is an Associate Editor of the IEEE/OSA JOURNAL OF LIGHTWAVE TECHNOLOGY and a Guest Editor of the IEEE JOURNAL OF SELECTED TOPICS IN QUANTUM ELECTRONICS issue on Solid-State Lighting in 2009. He received the Ta-You Wu Young Scholar Award from the National Science Council Taiwan in 2007 and the Young Photonics Researcher Award from OSA/SPIE Taipei chapter in 2007. He was elected as an OSA Fellow and the SPIE Fellow in 2012.
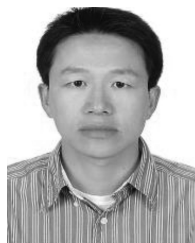
Jyehong Chen received the B.S. and M.S. degrees in electrical engineering from National Taiwan University, Taipei, Taiwan, in 1988 and 1990, respectively, and the Ph.D. degree in electrical engineering and computer science from the University of Maryland, Baltimore, MD, USA, in 1998.

He joined JDSU in 1998 as a Senior Engineer and obtained 10 U.S. patents in two years. He joined the faculty of National Chiao-Tung University, Hsinchu, Taiwan, 2003, where he is currently a Professor and the Director of the Institute of Electro-Optical Engineering and the Department of Photonics. He published more than 100 papers in international journals and conferences. His research interests include hybrid access network, long-reach passive optical network, and optical interconnects.